

## Parallel-Stacked Aromatic Hosts for Orienting Small Molecules in a Magnetic Field: Induced Residual Dipolar Coupling by Encapsulation

Sota Sato,<sup>\*,†</sup> Osamu Morohara,<sup>†</sup> Daishi Fujita,<sup>†</sup> Yoshiki Yamaguchi,<sup>‡</sup> Koichi Kato,<sup>§,||</sup> and Makoto Fujita<sup>\*,†,||</sup>

Department of Applied Chemistry, School of Engineering, The University of Tokyo, JST-CREST, 7-3-1 Hongo, Bunkyo-ku, Tokyo, 113-8656, Structural Glycobiology Team, RIKEN, Advanced Science Institute, 2-1 Hirosawa Wako, Saitama, 351-0198, Japan, Graduate School of Pharmaceutical Sciences, Nagoya City University, 3-1 Tanabe-dori, Mizuho-ku, Nagoya, 467-0027, and Okazaki Institute for Integrative Bioscience and Institute for Molecular Science, JST-CREST, 5-1 Higashiyama, Myodaiji, Okazaki, Aichi, 444-8787, Japan

Received January 13, 2010; E-mail: ssato@appchem.t.u-tokyo.ac.jp; mfujita@appchem.t.u-tokyo.ac.jp

Residual dipolar coupling (RDC) is the magnetically induced dipolar coupling of spin-active nuclei, which can be observed by NMR when molecules are anisotropically oriented in solution.<sup>1</sup> Since the RDC is a function of the angle defined by the vectors of the coupled nuclear dipoles and applied magnetic field, RDC values contain 3D structural information for the measured molecule. This modern NMR technique is increasingly important for elucidating the 3D structures of biomolecules but seldom applied to small molecules.<sup>2</sup>

$\pi$ -Conjugated molecules are, in principle, magnetically oriented and RDC active because there is a faint energy difference between parallel and perpendicular conformations with respect to the applied magnetic field.<sup>3</sup> However, this energy difference is extremely small and the RDC is detectable only for large aromatic molecules with extensive  $\pi$ -systems. Liquid crystals,<sup>4</sup> bicelles,<sup>1b,5</sup> and filamentous viruses<sup>6</sup> have been developed as polymeric alignment media to enhance the magnetic orientation of biomolecules but are not well-suited for small organic molecules due to weak interactions. We predict that, if an RDC silent molecule is tightly encapsulated in an oriented molecular host with multiple parallel-aligned  $\pi$ -systems, the target molecule will also be oriented within the host and become RDC active. And we now report that organic pillared cage **1** and interlocked cage **2** (Figure 1) composed of parallel, large aromatic ligands are RDC active and induce clearly detectable RDC for pyrene **3**, an RDC silent aromatic. We think of cages **1** and **2** as “magnetic aligners” and envision their application for the RDC structural analysis of small organic molecules.

RDC values are obtained by measuring the observed  $^1\text{H}$ – $^{13}\text{C}$   $J$  couplings at different magnetic field strengths: in the present study, 300 to 920 MHz NMR spectrometers, corresponding to 6.99 to 21.6 T, were used. The observed  $^1\text{H}$ – $^{13}\text{C}$  couplings are the sum of the invariable coupling constant ( $^1J_{\text{CH}}$ ) and RDC value ( $^1D_{\text{CH}}$ ). The relationship between  $^1D_{\text{CH}}$  and magnetic field strength,  $B$ , is given in eq 1, and magnetic orientation is thus indicated by a linear relationship between the observed coupling values and the square of the field strength,  $B^2$ .<sup>7</sup>

$$D_{\text{CH}} = -\frac{\gamma_{\text{C}}\gamma_{\text{H}}\hbar}{2\pi^2 r_{\text{CH}}^3} \left( \frac{3}{2} \cos^2 \theta - \frac{1}{2} \right) \frac{\Delta\chi}{15kT} B^2 \quad (1)$$

Coordination host **1**<sup>9</sup> consists of two parallel-aligned large aromatic panels (2,4,6-tri-4-pyridyltriazine) and three pyrazine

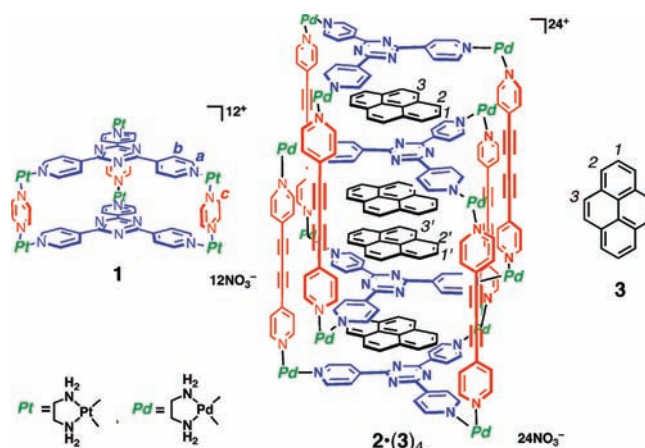


**Figure 1.** Structures of **1**–**3**. Positions of  $^1\text{H}$  and  $^{13}\text{C}$  nuclei ( $a$ – $c$ ,  $1$ – $3$ , and  $1'$ – $3'$ ) used for the RDC analysis are labeled.

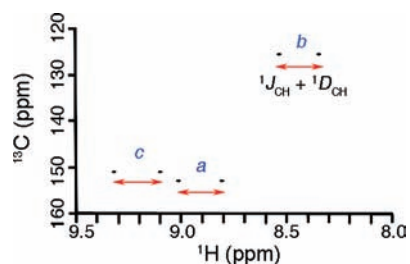


**Figure 2.**  $^{13}\text{C}$ -coupled  $^1\text{H}$ – $^{13}\text{C}$  HSQC spectrum of **1** (920 MHz,  $\text{D}_2\text{O}$ ).  $^1\text{H}$ – $^{13}\text{C}$  pairs  $a$ – $c$  are indicated in Figure 1.

pillars. For all  $^1\text{H}$ – $^{13}\text{C}$  pairs,  $a$ ,  $b$ , and  $c$  (Figure 1), the observed splitting values were obtained from the F2 axis in the  $^{13}\text{C}$ -coupled  $^1\text{H}$ – $^{13}\text{C}$  HSQC spectra (Figure 2). The  $^1J_{\text{CH}} + ^1D_{\text{CH}}$  values decreased with increasing field strengths, and natural  $^1J_{\text{CH}}$  values were determined by extrapolation to 0 T (Table 1).  $^1D_{\text{CH}}$  values

**Table 1.** Observed Couplings (Hz) for Host **1** and Extrapolated  $^1J_{\text{CH}}$  Constants (Hz)<sup>a</sup>

entry	observed coupling (Hz)				$^1J_{\text{CH}}$ (Hz)
	300 MHz (6.99 T) <sup>b</sup>	500 MHz (11.7 T) <sup>c</sup>	600 MHz (14.1 T) <sup>b</sup>	920 MHz (21.6 T) <sup>c</sup>	
$\text{H}^a\text{--C}^a$	188.4	188.1	187.8	187.1	188.5
$\text{H}^b\text{--C}^b$	174.3	173.9	173.7	172.8	174.4
$\text{H}^c\text{--C}^c$	198.2	198.2	198.0	197.8	198.2

<sup>a</sup> Extrapolated to 0 T. <sup>b</sup> Experimental error was 0.1 Hz. <sup>c</sup> Experimental error was 0.2 Hz.

<sup>†</sup> The University of Tokyo.

<sup>‡</sup> RIKEN.

<sup>§</sup> Nagoya City University, OIIB and IMS.

<sup>||</sup> JST-CREST.

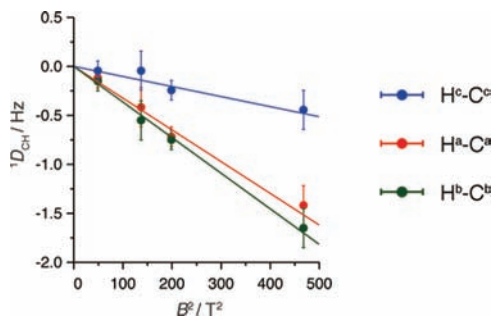


**Figure 3.** RDC ( $^1D_{\text{CH}}$ ) values plotted vs  $B^2$  for host **1**.

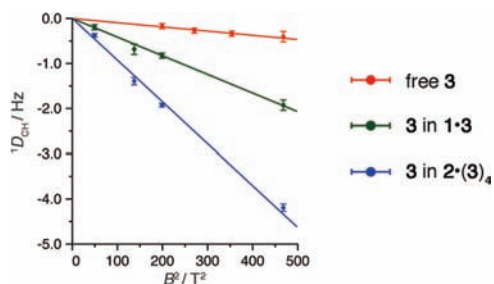


**Figure 4.** Observed  $^1D_{\text{CH}}$  vs  $B^2$  plot for **3** in dichloromethane (red) and in host-guest complexes **1**•**3** (green) and **2**•(**3**)<sub>4</sub> (blue). Average values for three (free **3**, **1**•**3**) and six H–C pairs (**2**•(**3**)<sub>4</sub>) are plotted.

showed good linear relationships with  $B^2$ , within the experimental error,<sup>10</sup> and clearly indicated that host **1** was magnetically orientated (Figure 3).

As eq 1 indicates, the magnetic susceptibility anisotropy ( $\Delta\chi$ ) that represents the degree of magnetic orientation can be evaluated from the slope of the linear fitting. Assuming that the molecular axis  $z$  is perpendicular to the largest aromatic plane,<sup>6a</sup>  $\theta = 90^\circ$  for the in-plane  $\text{H}^a\text{--C}^a$  and  $\text{H}^b\text{--C}^b$  pairs. Thus the slopes of  $D_{\text{CH}}$  vs  $B^2$  plots of both the  $a$  and  $b$  H–C pairs are nearly identical and gave  $\Delta\chi \approx -9 \times 10^{-28} \text{ cm}^3 \cdot \text{mol}^{-1}$ .

After demonstrating that cage **1** is oriented in a magnetic field and exhibits observable RDC, we examined the induced magnetic alignment of an encapsulated guest using pyrene **3**. The inclusion complex **1**•**3** was easily prepared by suspending powdered **3** in the aqueous solution of **1**. Within host **1** pyrene **3** was held in alignment with the magnetic field and RDCs were observed and showed good linear relationships with  $B^2$ . In host–guest complex **1**•**3**, guest **3** is held parallel to the plane of the triazine panels in host **1**, and all the  $\theta$  values for  $\text{H}^1\text{--C}^1$ ,  $\text{H}^2\text{--C}^2$ , and  $\text{H}^3\text{--C}^3$  pairs of **3** are also  $90^\circ$ ; the  $^1D_{\text{CH}}$  values for these pairs were accordingly identical (within experimental error) (Figure 4, green line). In contrast, the RDC for free pyrene (**3**) was negligible (Figure 4, red line). Thus, host **1** acted as a “magnetic aligner” for a small molecule.

The RDC of **3** was further enhanced upon encapsulation into interlocked cage **2**, with a greater number of parallel aromatic rings. The self-assembly of this multistack host–guest complex (**2**•(**3**)<sub>4</sub>) has been previously reported.<sup>11</sup> The slope of the  $^1D_{\text{CH}}$  vs  $B^2$  plot for **3** in **2**•(**3**)<sub>4</sub> (Figure 4, blue line) is significantly larger than that in **1**•**3**. The inner and outer pyrene guests in the **2**•(**3**)<sub>4</sub> complex are inequivalent, and the six H–C pairs are labeled as 1–3 and 1′–3′ (See Figure 1). The six pairs show identical  $^1D_{\text{CH}}$  values

(within experimental error) and are consistent with a parallel arrangement of the four molecules of **3** in the interspaces of host **2**.

In summary, we utilized discrete, self-assembled hosts with parallel aligned aromatic stacks as “magnetic aligners” to orient a small organic molecule in a magnetic field. Induced RDC was observed for the included guest molecule and promises that this new methodology of magnetic alignment with synthetic hosts can be further applied to the 3D structure determination of more complex guest molecules. This class of self-assembled coordination hosts is highly modular and well suited for the development of a new class of molecular magnetic aligners. Therefore, the reported methodology will serve as a structural determination tool for small molecules.<sup>2</sup>

**Acknowledgment.** This work was supported by Nanotechnology Network Project (A108, A124, and B106) and KAKENHI (20107004) of MEXT. We thank Dr. H. Sakakawa (IMS and JEOL) and Mr. H. Sato (Bruker Biospin) for the support of NMR pulse sequences.

**Note Added after ASAP Publication.** The definition of  $\theta$  was corrected on March 17, 2010.

**Supporting Information Available:** Experimental details, NMR spectra, and processing and analysis of NMR data. This material is available free of charge via the Internet at <http://pubs.acs.org>.

## References

- (1) (a) Prestegard, J. H. *Proc. Natl. Acad. Sci. U.S.A.* **1995**, *92*, 9279–9283. (b) Tolman, J. R.; Flanagan, J. M.; Kennedy, M. A.; Tjandra, N.; Bax, A. *Science* **1997**, *278*, 1111–1114. (c) Tjandra, N.; Omichinski, J. G.; Gronenborn, A. M.; Clore, G. M.; Bax, A. *Nat. Struct. Biol.* **1997**, *4*, 732–738. (d) Tolman, J. R.; Flanagan, J. M.; Kennedy, M. A.; Prestegard, J. H. *Nat. Struct. Biol.* **1997**, *4*, 292–297. (e) Prestegard, J. H.; Hashimi, H. M.; Tolman, J. R. *Q. Rev. Biophys.* **2000**, *33*, 371–424. (f) de Alba, E.; Tjandra, N. *Prog. NMR Spectrosc.* **2002**, *40*, 175–197.
- (2) (a) Van Zijl, P. C. M.; Ruessink, B. H.; Bultuis, J.; MacLean, C. *Acc. Chem. Res.* **1984**, *17*, 172–180. (b) Suryaprakash, N. *Concepts Magn. Reson.* **1998**, *10*, 167–192. (c) Yan, J.; Zartler, E. R. *Magn. Reson. Chem.* **2005**, *43*, 53–64. (d) Thiele, C. M. *Concept Magn. Reson. A* **2007**, *30A*, 65–80. (e) Jin, L.; Pham, T. N.; Uhrin, D. *ChemPhysChem* **2007**, *8*, 1228–1235. (f) Thiele, C. M. *Eur. J. Org. Chem.* **2008**, *567*, 3–5685. (g) Kummerlöwe, G.; Luy, B. *Trends Anal. Chem.* **2009**, *28*, 483–493.
- (3) (a) Lohman, J. A. B.; MacLean, C. *Chem. Phys.* **1978**, *35*, 269–274. (b) Gayathri, C.; Bothner-By, A. A.; Van Zijl, P. C. M.; Maclean, C. *Chem. Phys. Lett.* **1982**, *87*, 192–196. (c) Lisicki, M. A.; Mishra, P. K.; Bothner-By, A. A.; Lindsey, J. S. *J. Phys. Chem.* **1988**, *92*, 3400–3403. (d) Alemany, L. B.; Gonzalez, A.; Billups, W. E.; Willcott, M. R.; Ezell, E.; Gonzansky, E. *J. Org. Chem.* **1997**, *62*, 5771–5779. (e) van Buuren, B. N. M.; Schleucher, J.; Wittmann, V.; Griesinger, C.; Schwalbe, H.; Wijmenga, S. S. *Angew. Chem., Int. Ed.* **2004**, *43*, 187–192.
- (4) (a) Saupé, A.; Englert, G. *Phys. Rev. Lett.* **1963**, *11*, 462–464. (b) Prosser, S. R.; Losonczy, J. A.; Shiyonovskaya, I. V. *J. Am. Chem. Soc.* **1998**, *120*, 11010–11011.
- (5) (a) Sanders, C. R.; Prestegard, J. H. *Biophys. J.* **1990**, *58*, 447–460. (b) Sanders, C. R.; Schwonek, J. P. *Biochemistry* **1992**, *31*, 8898–8905.
- (6) (a) Hansen, M. R.; Mueller, L.; Pardi, A. *Nat. Struct. Biol.* **1998**, *5*, 1065–1074. (b) Clore, G. M.; Starich, M. R.; Gronenborn, A. M. *J. Am. Chem. Soc.* **1998**, *120*, 10571–10572.
- (7)  $\theta$ : the angle between the molecular axis  $z$ , perpendicular to the aromatic plane, and coupled C–H vector.  $\Delta\chi$ : magnetic susceptibility anisotropy.  $\gamma_C$  and  $\gamma_H$ : the gyromagnetic ratio of nuclei  $^{13}\text{C}$  and  $^1\text{H}$ , respectively.  $h$ : Planck’s constant.  $r_{\text{CH}}$ : the internuclear distance (1.09 Å for aromatic CH).<sup>8</sup>
- (8) Pliva, J.; Johns, J. W. C.; Goodman, L. *J. Mol. Spectrosc.* **1991**, *148*, 427–435.
- (9) Kumazawa, K.; Biradha, K.; Kusukawa, T.; Okano, T.; Fujita, M. *Angew. Chem., Int. Ed.* **2003**, *42*, 3909–3913.
- (10) The experimental error values were derived from the digital resolution settings. See: Yan, J.; Kline, A. D.; Mo, H.; Shapiro, M. J.; Zartler, E. R. *J. Org. Chem.* **2003**, *68*, 1786–1795.
- (11) (a) Yamauchi, Y.; Yoshizawa, M.; Fujita, M. *J. Am. Chem. Soc.* **2008**, *130*, 5832–5833. (b) Klosterman, J. K.; Yamauchi, Y.; Fujita, M. *Chem. Soc. Rev.* **2009**, *38*, 1714–1725.

JA100325B